Title:
Cocrystal trimorphism as a consequence of orthogonality of halogen- and hydrogen-bonds synthons

Authors:
Filip Topić,[a,b] Katarina Lisac,[b,c] Mihails Arhangelskis,[a] Kari Rissanen[b,*], Dominik Cinčić[c,*] and Tomislav Friščić[a,*]

Author address:
a) Department of Chemistry, McGill University, 801 Sherbrooke St. W., H3A 0B8, Montreal, Canada; b) Department of Chemistry, University of Jyvaskyla, P.O. Box 35, FI-40014, Finland; c) Department of Chemistry, Faculty of Science, University of Zagreb, Horvatovac 102a, HR-10000, Zagreb, Croatia.

Abstract:
True trimorphic cocrystals, i.e. multi-component molecular crystals of identical composition that exhibit three polymorphic structures, are exceedingly rare and so far no halogen-bonded cocrystal system was reported to exhibit trimorphism. Here, we describe a unique example of a trimorphic cocrystal exhibiting both hydrogen and halogen bonds in which the difference between polymorphs arises from their orthogonality evident by apparently independent variation of hydrogen- and halogen-bonded motifs.

Main text:
Over the past decade, cocrystallisation[1] has developed into an established crystal engineering strategy to generate new molecular solids with notable optical,[2] pharmaceutical,[3–5] energetic[6–8] or otherwise stimuli-responsive[9] properties. Cocrystal design relies on well-defined, robust motifs of intermolecular interactions, supramolecular synthons, driving the assembly of molecular components in a predictable manner.[10–12] In that context, polymorphism in cocrystals is still a poorly investigated challenge,[13–15] especially when different cocrystal polymorphs exhibit a different arrangement of intermolecular interactions.

Here, we describe a trimorphic cocrystal system in which polymorphism stems from orthogonality of halogen- (XB) and/or hydrogen-bonding (HB) interactions. Orthogonality is a well-established concept in organic synthesis and covalent self-assembly, enabling the synthesis of complex targets and the design of one-pot and cascade synthetic strategies.[16] In solid-state supramolecular chemistry, orthogonality has been recognized as critical for the controlled assembly of complex structures from small molecule components, either *via* covalent bonds[17] or non-covalent interactions.[18] We now report orthogonality of supramolecular interactions as a basis of cocrystal polymorphism, with structural differences between herein reported three cocrystal polymorphs readily described by independent variation in XB and HB motifs. While dimorphic cocrystals, exhibiting two polymorphic modifications, are well-known,[19–22] the number of reported cocrystals with three (trimorphic cocrystals) or more polymorphs is much smaller,[4,23–25] making the herein reported system of particular interest. Importantly, so far there have been no reports of cocrystal trimorphism involving halogen bonds, which is of potentially broader importance due to interest in XB research[26] in the design of functional[27,28] (e.g. pharmaceutical)

cocrystals.[29,30] Finally, this study establishes, to the best of our knowledge, a record of five crystalline phases in a halogen-bonded cocrystal system, including three polymorphs, one stoichiometric variation[31] (stoichiomorph[32]), and an acetonitrile solvate.[33]

We have previously reported that cocrystallisation of 1,4-diiodotetrafluorobenzene (**tfib**) as an XB donor with methyldiphenylphosphine oxide (**mdppo**) as the acceptor (Scheme 1)[31] forms two stoichiometrically different[20] cocrystals (**mdppo**)(**tfib**) (CSD LICBEG) and (**mdppo**)$_2$(**tfib**) (CSD LICBIK).

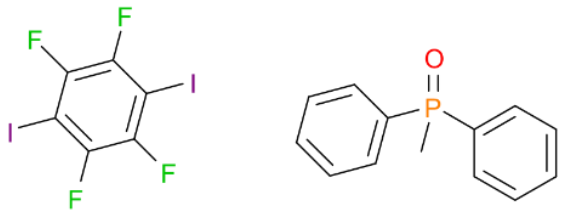

tfib **mdppo**

Scheme 1. Structural formulas of **tfib** and **mdppo**.

In (**mdppo**)(**tfib**), each **tfib** molecule was found to engage in one I···O and one I···π interaction with a **mdppo** phenyl ring. Unexpectedly, the I···O halogen bonds were absent in the structure of (**mdppo**)$_2$(**tfib**). Instead, structure exhibited both iodine atoms of **tfib** engaged in I···π interactions[34] (Fig. 1a), along with the formation of C–H···O HB tapes between neighbouring **mdppo** units (Fig. 2a). The absence of I···O bonds was particularly unexpected, as using octafluoro-1,4-diiodobutane (**ofib**, an aliphatic XB donor of similar length to **tfib**) gave a (**mdppo**)$_2$(**ofib**) cocrystal with each donor engaged in two I···O halogen bonds (CSD GIDRES).[31]

In the course of our work on synthesizing ternary cocrystals through combining mutually orthogonal interactions,[18] we now report serendipitous discovery of two new polymorphs of (**mdppo**)$_2$(**tfib**). The cocrystals were unexpectedly isolated from a solution of **mdppo**, **tfib** and *N*,*N'*-dimethylthiourea in acetonitrile. Crystal structure determination revealed that, unlike the previously reported cocrystal of orthorhombic (*ortho*) symmetry, the two new (**mdppo**)$_2$(**tfib**) forms crystallize in the monoclinic (*mono*) and triclinic (*tric*) crystal systems. The *ortho*-, *mono*- and *tric*-forms of (**mdppo**)$_2$(**tfib**) represent a so far unique trimorphic set of halogen-bonded cocrystals. Specifically, we were surprised[35] to find that the I···O halogen bonds, absent in *ortho*-(**mdppo**)$_2$(**tfib**), are now present in both *mono*- and *tric*-(**mdppo**)$_2$(**tfib**). In *mono*-(**mdppo**)$_2$(**tfib**) (Fig. 1b), each XB donor molecule forms two symmetrically equivalent I···O halogen bonds, with a distance of $d_{I\cdots O}$ = 2.815(1) Å (R_{XB} = 0.804) and an angle $<_{C-I\cdots O}$ = 171.50(6)°. Similarly, *tric*-(**mdppo**)$_2$(**tfib**) (Fig. 1c) again displays two symmetrically equivalent I···O halogen bonds per each **tfib** molecule, with $d_{I\cdots O}$ = 2.837(2) Å (R_{XB} = 0.811) and $<_{C-I\cdots O}$ = 175.6(1)°. These values are similar to those for the (**mdppo**)$_2$(**ofib**) ($d_{I\cdots O}$ = 2.809(1) Å, R_{XB} = 0.803, $<_{C-I\cdots O}$ = 173.14(6)°).

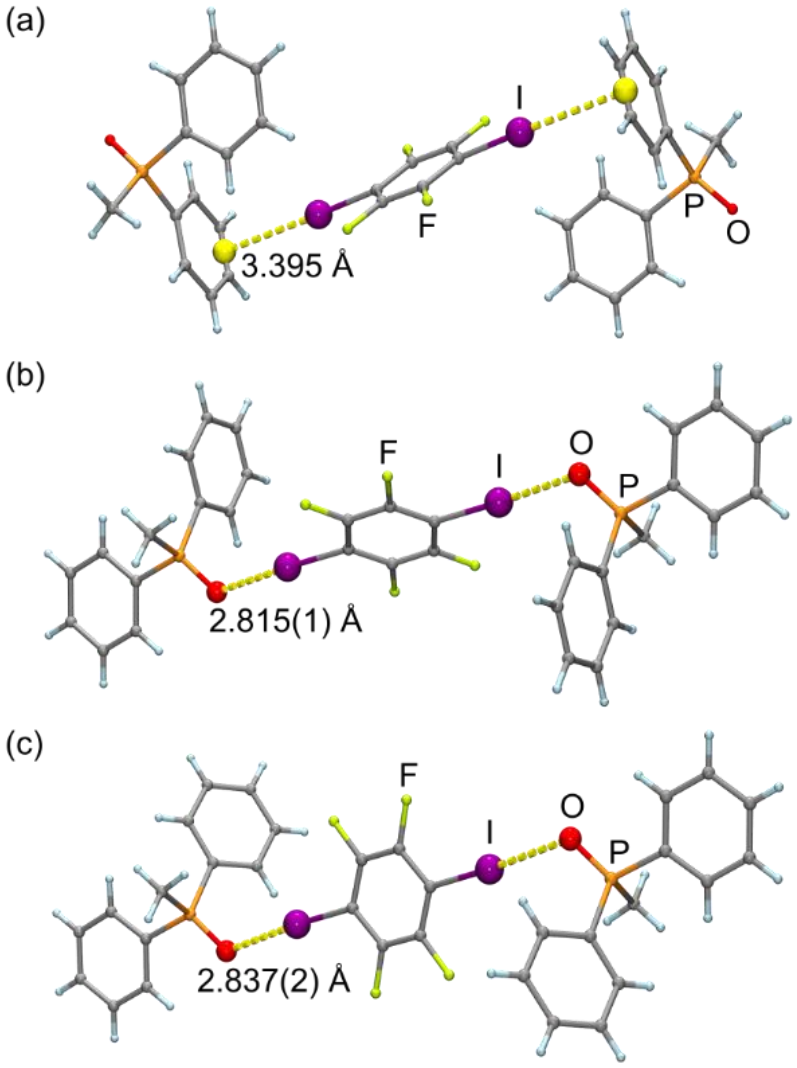

Figure 1. Halogen-bonded assemblies in a) *ortho*-(**mdppo**)$_2$(**tfib**), based on I···π XBs, and in b) *mono*-(**mdppo**)$_2$(**tfib**) and c) *tric*-(**mdppo**)$_2$(**tfib**), based on I···O XBs.

Structures of *mono*- and *tric*-(**mdppo**)$_2$(**tfib**) also exhibit tape-like C−H···O networks, similar to those in the *ortho*-polymorph (Fig. 2). Importantly, *mono*-(**mdppo**)$_2$(**tfib**) exhibits a HB motif composed of two antiparallel $C(4)$ chains and $R_3^2(8)$ rings, identical to that seen in *ortho*-(**mdppo**)$_2$(**tfib**) (Fig. 2a), as well as in the previously reported (**mdppo**)$_2$(**ofib**) and in solid **mdppo**, whose structure has herein been re-determined at 123 K to facilitate comparison of HB patterns (for previous structural report, see CSD NEXBOI).[36] The $C(4)R_3^2(8)$ pattern in *mono*-(**mdppo**)$_2$(**tfib**) is generated *via* a twofold 2_1 screw axis (Fig. 2d), similar to that in (**mdppo**)$_2$(**ofib**), and in contrast to *ortho*-(**mdppo**)$_2$(**tfib**) and solid **mdppo**, where this motif arises as a result of glide planes (Fig. 2b). This leads to a difference in relative orientation of phenyl rings on neighboring **mdppo** molecules: in *ortho*-(**mdppo**)$_2$(**tfib**) the phenyl groups are all located on the same side of the C–H···O tape, whereas in *mono*-(**mdppo**)$_2$(**tfib**) their positioning alternates on both sides of the supramolecular tapes (Figs. 2b,d). The C–H···O distances in *ortho*- and *mono*-(**mdppo**)$_2$(**tfib**) are highly similar, from 3.308(5) Å to 3.377(5) Å (Table 1), which is close to values seen in the (**mdppo**)$_2$(**ofib**) cocrystal and pure **mdppo**.

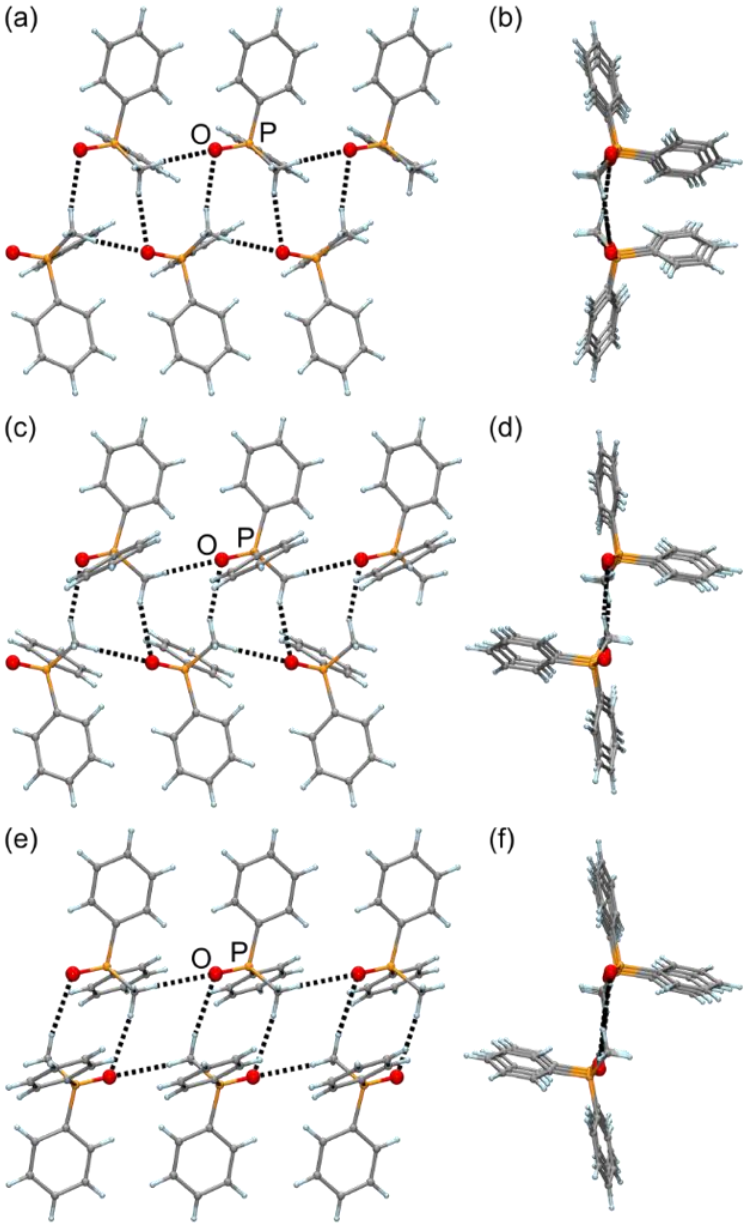

Figure 2. Two different views (normal and parallel to the direction of tape propagation) of HB tape motifs in the trimorphic cocrystals: a-b) $C(4)$ $R_3^2(8)$ motif in *ortho*-(**mdppo**)$_2$(**tfib**); c-d) $C(4)$ $R_3^2(8)$ motif in *mono*-(**mdppo**)$_2$(**tfib**); e-f) C(4) $R_2^2(8)$ $R_4^2(8)$ motif in *tric*-(**mdppo**)$_2$(**tfib**).

In contrast, C−H···O interactions in *tric*-(**mdppo**)$_2$(**tfib**) exhibit a different $C(4)R_2^2(8)$ first-order and $R_4^2(8)$ second-order network (Fig. 2e). This pattern, which is a phosphine oxide analogue of the "amide ladder" motif,[37] is generated in this cocrystal by the inversion centres of the $P\bar{1}$ space group. The appearance of a different HB pattern in *tric*-(**mdppo**)$_2$(**tfib**) is accompanied by a notable elongation of C−H···O bonds compared to other polymorphs and the structures of (**mdppo**)$_2$(**ofib**) and **mdppo**, with C···O separations now being effectively longer than 3.5 Å (Table 1).

Attempts at selective mechanochemical synthesis of *mono*-(**mdppo**)$_2$(**tfib**) and *tric*-(**mdppo**)$_2$(**tfib**) were not successful, with neat and liquid-assisted grinding[38] respectively

producing mixtures of *tric*- and *ortho*-(**mdppo**)$_2$(**tfib**) or just *ortho*-(**mdppo**)$_2$(**tfib**). Subsequently, reliable procedures were devised for selective solution synthesis of the two new polymorphs.

Table 1. Comparison of the patterns, distances (*d*, in Å) and angles (α, in °) of C−H···O HBs between phosphorus-bound methyl and oxygen groups in three forms of (**mdppo**)$_2$(**tfib**), as well as (**mdppo**)$_2$(**ofib**) and **mdppo**.

Compound	Pattern	*d* / Å	α / °
ortho-(**mdppo**)$_2$(**tfib**)[31,a]	$C(4)R_3^2(8)$	3.308(5) 3.377(5)	172.9 162.7
mono-(**mdppo**)$_2$(**tfib**)[b]	$C(4)R_3^2(8)$	3.335(2) 3.339(3)	151.7 150.8
tric-(**mdppo**)$_2$(**tfib**)[b]	$C(4)R_2^2(8)$ $R_4^2(8)$	3.540(5) 3.501(4)	160.3 158.3
(**mdppo**)$_2$(**ofib**)[32,c]	$C(4)R_3^2(8)$	3.318(2) 3.370(2)	145.5 147.1
mdppo[36,a]	$C(4)R_3^2(8)$	3.312(2) 3.325(2) 3.391(2) 3.485(2) 3.359(2) 3.321(2)	166.7 173.6 168.1 163.1 162.2 163.7

a) re-determined at 123 K; b) measured at 123 K; c) at 180 K.

First, **mdppo** and **tfib**, in a 2:1 stoichiometric ratio, were dissolved in a small amount of *iso*-butanol with the help of an ultrasound bath and left to stand at room temperature. After one hour, the resulting crystals were filtered off and identified as *mono*-(**mdppo**)$_2$(**tfib**). Placing a similarly prepared solution into a freezer at ca. −20 °C for 10 days yielded crystals of *tric*-(**mdppo**)$_2$(**tfib**). Sample purity was confirmed by powder X-ray diffraction (PXRD, Fig. 3). It is unclear why certain conditions lead to selective formation of different (**mdppo**)$_2$(**tfib**) polymorphs. We believe that solvent might play a significant role – a view reinforced by prior observation of a 3-component solvate of the (**mdppo**)(**tfib**) cocrystal from acetonitrile (CSD JUZSAA).[33]

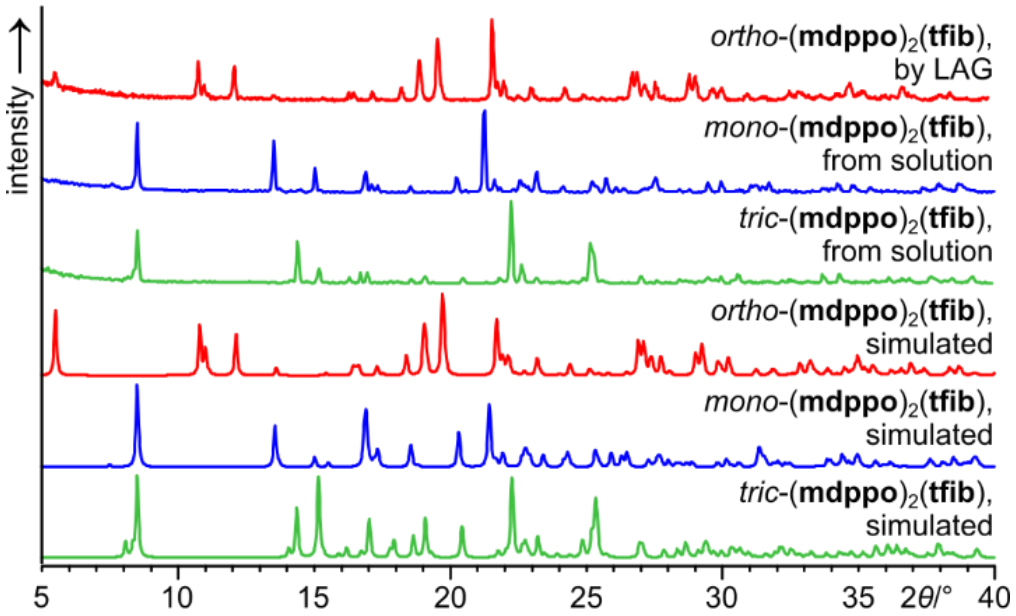

Figure 3. Comparison of the experimental and simulated powder patterns for the separately synthesized samples of the three polymorphs of (**mdppo**)$_2$(**tfib**).‡

Availability of pure *ortho*-, *tric*- and *mono*-(**mdppo**)$_2$(**tfib**) samples enabled a study of their stability by differential scanning calorimetry (DSC, Fig. 4). The DSC thermogram of *mono*-(**mdppo**)$_2$(**tfib**) was mostly featureless, exhibiting only a sharp endothermic event at ca. 113 °C, consistent with melting. In contrast, heating of *tric*- or *ortho*-polymorphs led to a broad endothermic feature at ca. 86 or 96 °C, respectively, followed by a sharp endothermic melting signal at ca. 113 °C. These observations indicate that *mono*-(**mdppo**)$_2$(**tfib**) is the thermodynamically preferred form at elevated temperature, with both *ortho*- and *tric*-forms first undergoing a transformation to *mono*-(**mdppo**)$_2$(**tfib**), which melts at 113 °C.

Relative stabilities of (**mdppo**)$_2$(**tfib**) forms were also investigated computationally, by periodic density functional theory (DFT) calculations using CRYSTAL17[39] with a range-separated ωB97X functional,[40] previously successfully used to rationalize stability of XB cocrystals.[41] All-electron basis sets, specifically adapted for periodic calculations, were implemented for H, C, O, F and P,[42] and effective core potentials[43] were used to account for relativistic effects in I.[44] Lattice energy calculations on the DFT-optimised structures of the three polymorphs of (**mdppo**)$_2$(**tfib**) revealed that *ortho*-(**mdppo**)$_2$(**tfib**) should be the most stable one, with *mono*-(**mdppo**)$_2$(**tfib**) and *tric*-(**mdppo**)$_2$(**tfib**) higher in energy by +7.67 kJ mol^{-1} and +7.87 kJ mol^{-1}, respectively. These results are consistent with persistence of *ortho*-(**mdppo**)$_2$(**tfib**) as the only or the major product in most solution and mechanochemical experiments, and with the endothermic nature of the transformation from *ortho*- to *mono*-(**mdppo**)$_2$(**tfib**).

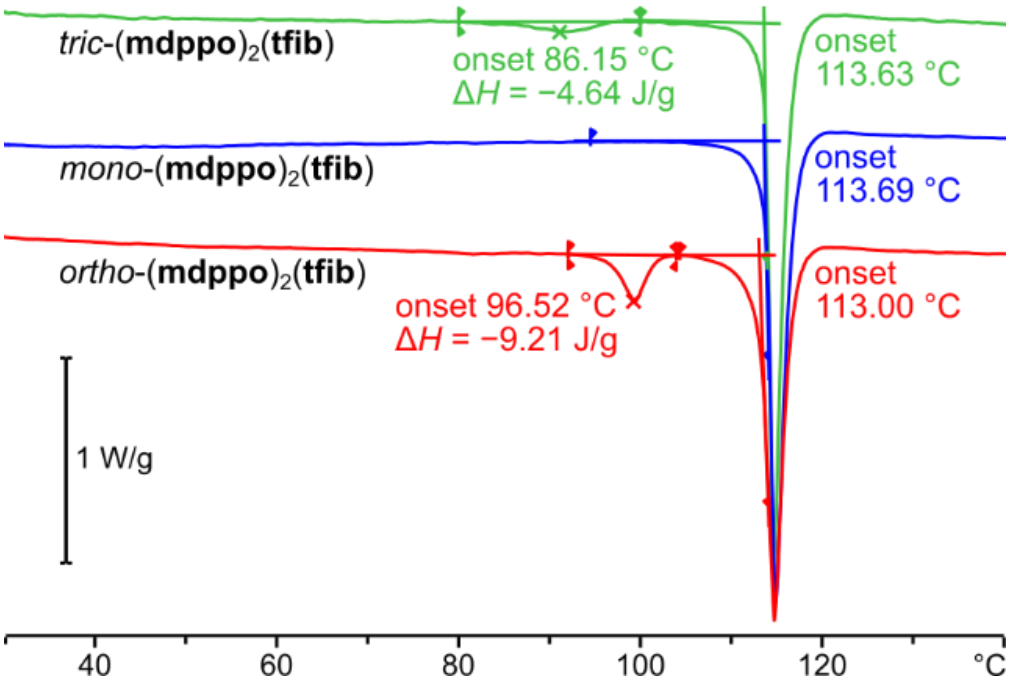

Figure 4. Comparison of the DSC thermograms for three polymorphs of (**mdppo**)$_2$(**tfib**), recorded at heating rate of 5 K/min in a N_2 flow atmosphere.

Trimorphism of (**mdppo**)$_2$(**tfib**) is unique among XB cocrystals, as a search of the Cambridge Structural Database revealed only 12 cases of polymorphism (all dimorphic) in over 900 structures of multi-component crystals involving perfluorinated XB donors (see ESI). Comparison of the three forms of (**mdppo**)$_2$(**tfib**) suggests an important role for orthogonality of supramolecular interactions in generating the observed polymorphs. Specifically, the three polymorphs can be seen as related by single independent changes in either HB or XB patterns (Scheme 2). In such a scheme, *mono*-(**mdppo**)$_2$(**tfib**) adopts a special place, as both the *ortho*- and *tric*-forms can be envisaged as being generated from it, either by variation of XB motifs without affecting the HB theme, or by changes in HB pattern without significant changes to XB, respectively.

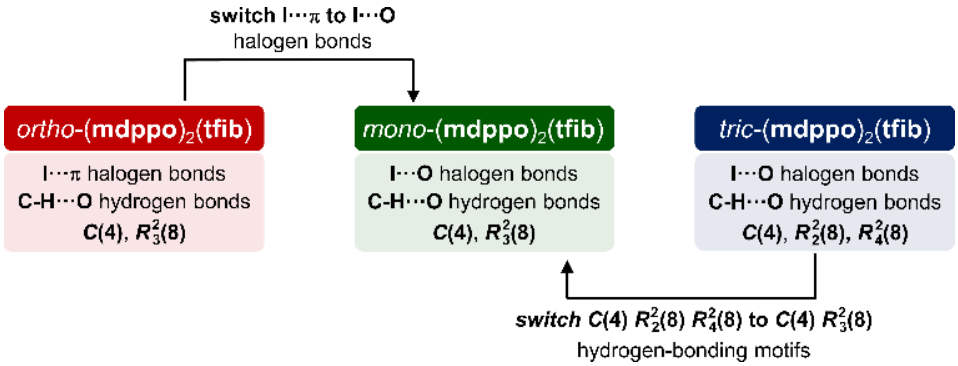

Scheme 2. Relationship between XB and HB motifs in polymorphs of (**mdppo**)$_2$(**tfib**).

In summary, we presented a unique example of a trimorphic cocrystal based on halogen bonds. Importantly, a potential role of orthogonality of supramolecular interactions in polymorphism of cocrystals is revealed, as the three reported structures can be mutually related by individual and

independent variation in either XB or HB patterns. The presented trimorphism contributes to unique richness of five phases for this halogen-bonded system, which now includes three polymorphs of (**mdppo**)$_2$(**tfib**), a (**mdppo**)(**tfib**) stoichiomorph,[32] and a solvate (**mdppo**)(**tfib**)(CH_3CN).[33] While orthogonality of supramolecular interactions has typically been regarded as a design element in the synthesis of complex structures, these results also suggest orthogonality as a route to extended polymorphism. We are currently investigating other chemically similar systems for further cases of polymorphism based on orthogonality of supramolecular interactions.

Conflicts of interest:

There are no conflicts to declare.

Notes:

‡For easier comparison of simulated and experimental patterns, structure of *tric*-(**mdppo**)$_2$(**tfib**) was also determined at 253 K.

References:

1 C. Aakeröy, *Acta Crystallogr. B*, 2015, **71**, 387.
2 J.-C. Christopherson, F. Topić, C. J. J. Barrett and T. Friščić, *Cryst. Growth Des.*, 2018, **18**, 1245.
3 N. Schultheiss and A. Newman, *Cryst. Growth Des.*, 2009, **9**, 2950.
4 G. Bolla and A. Nangia, *Chem. Commun.*, 2016, **52**, 8342.
5 M. Karimi-Jafari, L. Padrela, G. M. Walker and D. M. Croker, *Cryst. Growth Des.*, 2018, **18**, 6370.
6 O. Bolton and A. J. Matzger, *Angew. Chem. Int. Ed.* 2011, **50**, 8960.
7 K. B. Landenberger, O. Bolton and A. J. Matzger, *J. Am. Chem. Soc.*, 2015, **137**, 5074.
8 J. Zhang and J. M. Shreeve, *CrystEngComm*, 2016, **18**, 6124.
9 O. S. Bushuyev, T. C. Corkery, C. J. Barrett and T. Friščić, *Chem. Sci.*, 2014, **5**, 3158.
10 G. R. Desiraju, *Angew. Chem. Int. Ed. English*, 1995, **34**, 2311.
11 C. A. Gunawardana and C. B. Aakeröy, *Chem. Commun.*, 2018, **54**, 14047.
12 M. K. Corpinot and D. K. Bučar, *Cryst. Growth Des.*, 2019, **19**, 1426.
13 S. Aitipamula, P. S. Chow and R. B. H. Tan, *CrystEngComm*, 2014, **16**, 3451.
14 S. Aitipamula, in *Advances in Organic Crystal Chemistry*, Springer Japan, Tokyo, 2015, pp. 265–298.
15 K. Kersten, R. Kaur and A. Matzger, *IUCrJ*, 2018, **5**, 124.
16 C.-H. Wong and S. C. Zimmerman, *Chem. Commun.*, 2013, **49**, 1679.
17 M. Pascu, A. Ruggi, R. Scopelliti and K. Severin, *Chem. Commun.*, 2013, **49**, 45.
18 F. Topić and K. Rissanen, *J. Am. Chem. Soc.*, 2016, **138**, 6610.
19 N. J. Babu, L. S. Reddy, S. Aitipamula and A. Nangia, *Chem. Asian J.*, 2008, **3**, 1122.
20 K. Raatikainen and K. Rissanen, *CrystEngComm*, 2009, **11**, 750.
21 M. D. Eddleston, S. Sivachelvam and W. Jones, *CrystEngComm*, 2013, **15**, 175.
22 R. Puttreddy, F. Topić, A. Valkonen and K. Rissanen, *Crystals*, 2017, **7**, 214.

23 T. Ueto, N. Takata, N. Muroyama, A. Nedu, A. Sasaki, S. Tanida and K. Terada, *Cryst. Growth Des.*, 2012, **12**, 485.
24 S. Aitipamula, P. S. Chow and R. B. H. Tan, *CrystEngComm*, 2009, **11**, 1823.
25 D. Braga, G. Palladino, M. Polito, K. Rubini, F. Grepioni, M. R. Chierotti and R. Gobetto, *Chem. Eur. J.*, 2008, **14**, 10149.
26 G. Cavallo, P. Metrangolo, R. Milani, T. Pilati, A. Priimagi, G. Resnati and G. Terraneo, *Chem. Rev.*, 2016, **116**, 2478.
27 M. A. Sinnwell and L. R. MacGillivray, *Angew. Chem. Int. Ed.*, 2016, **55**, 3477.
28 E. Bosch, S. J. Kruse, H. R. Krueger and R. H. Groeneman, *Cryst. Growth Des.*, 2019, **19**, 3092.
29 M. Baldrighi, G. Cavallo, M. R. Chierotti, R. Gobetto, P. Metrangolo, T. Pilati, G. Resnati and G. Terraneo, *Mol. Pharm.*, 2013, **10**, 1760.
30 D. Choquesillo-Lazarte, V. Nemec and D. Cinčić, *CrystEngComm*, 2017, **19**, 5293.
31 S. Y. Oh, C. W. Nickels, F. Garcia, W. Jones and T. Friščić, *CrystEngComm*, 2012, **14**, 6110.
32 M. Singh and D. Chopra, *Cryst. Growth Des.*, 2018, **18**, 6670.
33 Y. Xu, J. Viger-Gravel, I. Korobkov and D. L. Bryce, *J. Phys. Chem. C*, 2015, **119**, 27104.
34 E. Bosch and IUCr, *IUCrData*, 2019, **4**, x190993.
35 M. K. Corpinot, S. A. Stratford, M. Arhangelskis, J. Anka-Lufford, I. Halasz, N. Judaš, W. Jones and D.-K. Bučar, *CrystEngComm*, 2016, **18**, 5434.
36 F. Dornhaus, M. Bolte, H.-W. Lerner and M. Wagner, *Eur. J. Inorg. Chem.*, 2006, 5138.
37 C. B. Aakeröy, B. M. T. Scott and J. Desper, *New J. Chem.*, 2007, **31**, 2044.
38 T. Friščić, C. Mottillo and H. M. Titi, *Angew. Chem. Int. Ed.* 2019 DOI:10.1002/anie.201906755.
40 R. Dovesi, A. Erba, R. Orlando, C. M. Zicovich-Wilson, B. Civalleri, L. Maschio, M. Rérat, S. Casassa, J. Baima, S. Salustro and B. Kirtman, *Wiley Interdiscip. Rev. Comput. Mol. Sci.*, 2018, **8**, e1360.
41 J.-D. Chai and M. Head-Gordon, *J. Chem. Phys.*, 2008, **128**, 084106.
42 K. Lisac, F. Topić, M. Arhangelskis, S. Cepić, P. A. Julien, C. W. Nickels, A. J. Morris, T. Friščić and D. Cinčić, *Nat. Commun.*, 2019, **10**, 61.
43 M. F. Peintinger, D. V. Oliveira and T. Bredow, *J. Comput. Chem.*, 2013, **34**, 451.
44 K. A. Peterson, B. C. Shepler, D. Figgen and H. Stoll, *J. Phys. Chem. A*, 2006, **110**, 13877.
45 J. Laun, D. Vilela Oliveira and T. Bredow, *J. Comput. Chem.*, 2018, **39**, 1285.